

Fixed-Time Multi-UAV Collaborative Fault-Tolerant Formation Control for Sensor/Actuator Faults

Kun Liu, Jiayi Zheng, and Shulong Zhao

Abstract—In this research, a fixed-time cooperative fault-tolerant control (CFTC) protocol for multiple unmanned aerial vehicles (UAVs) formation is proposed. First, the assumption that faults are bounded is removed. A fixed-time observer (FTO) is utilized to estimate the pitot tube and actuator faults, which ensures that the estimation errors of the faults converge in a fixed time. Second, the norm-normalized sign function (NNSF) is introduced to make the control output change smoother and reduce the influence of faults, while simplifying the proof process. Finally, numerical simulations demonstrate the superior performance of the proposed CFTC compared to the existing work.

I. INTRODUCTION

Recently, Unmanned Aerial Vehicles (UAVs) have been used extensively in the domains of disaster assistance [1], collision avoidance [2], and target encirclement [3]. However, various complex environments and uncertainties would be encountered in these missions, such as the icing on the pitot tube, blockage of the air intake, and mechanical fault of the engine, which seriously affect UAV's capabilities. These problems may result in mission failure or even crashes [4]. Therefore, it is of significance to enhance the stability and security of unmanned aerial vehicles (UAVs) to ensure the successful execution of their missions in complex environments.

Fault-tolerant control (FTC) is an effective method to deal with faults of the UAV. FTC was primarily based on threshold setting to determine the occurrence of faults. McCloy et al. [5] devised a control scheme for tracking a restricted linear variable-parameter system to compensate for sensor faults, subject to a fixed threshold. Wang et al. adopted a model-free approach and designed a dynamic threshold for FTC to adjust the threshold parameter more easily [6], based on stability analysis, but the introduction of the dynamic threshold would lead to the sensitivity of fault detection. More recently, relying on a fixed-wing UAV dynamics model, Abbaspour et al. [7] designed a dynamic threshold for the FTC algorithm by a neural network and extended Kalman filter employed to estimate the threshold in real time.

The dynamic threshold is suitable to handle sensor faults due to its adaptability, but it poses challenges when addressing actuator faults. Gao et al. [8] designed an adaptive sliding mode controller (SMC), employing neural networks

to cope with actuator faults that may be encountered during UAV flights. Wang et al. [9] regarded actuator faults as unknown terms and directly used a fuzzy logic system (FLS) to compensate. Based on this, Han et al. [10] utilized the FLS to address sensor and actuator faults, respectively.

With the progress of related techniques, the application scenarios of UAVs are becoming more and more complicate. In particular, there is a growing demand for multi-UAV to implement missions coordinately. Nevertheless, cooperative control requires higher reliability and fault tolerance, and designing cooperative faults-tolerant control (CFTC) protocol is an alternative option. For the CFTC of multi-UAV formation, there are two main technological route, i.e., active and passive. Active CFTC focuses on selecting appropriate control strategies through accurate fault estimation. Yang et al. [11] proposed an adaptive iterative learning observer and utilized a terminal SMC to deal with the actuator fault. Liu et al. [12] used a fast adaptive fault estimation observer to estimate the faults and proposed an SMC to perform a distributed formation tracking. A distributed active CFTC method [13] is also designed subject to communication delays, external disturbance, and multiple faults. Compared with the active CFTC, the passive CFTC has a better robustness and does not need to distinguish the type of faults in advance, which has broader applications. Cheng et al. considered passive CFTC with external disturbances for actuator faults encountered in multi-UAV formation control based on the fixed-time theory [14]. A scheme was further designed to realize the CFTC with the prescribed performance [15]. Li et al. expanded the number of actuator faults and proposed an adaptive CFTC strategy for time-varying formations to effectively compensate for infinite uncertainty about the effects of actuator faults [16]. Han et al. proposed a distributed adaptive finite-time CFTC for sensor and actuator faults [17]. The above researches provide valuable guidance and essential references for the CFTC of UAV formation. However, the above methods can only deal with single fault cases [12]-[16] or bounded multiple-fault cases [17].

Most faults have an episodic character that generate a step response to the controller output, producing undesired jitter, especially under controllers with sign function [18]–[20]. The output of sign function is more prone to discontinuities, which may lead to fluctuations in the system performance. Compared to the classical sign function, the norm-normalized sign function (NNSF) is usually continuous, which makes it easier to achieve a smooth controller output [21]. Yan et al. applied the NNSF to UAV formation tracking with energy constraints [22]. Cheng et al. introduced

*This work was not supported by any organization.

Kun Liu, Jiayi Zheng, and Shulong Zhao are with College of Intelligence Science and Technology, National University of Defense Technology, Changsha, 410000, China (Corresponding author: Shulong Zhao) liukun222@nudt.edu.cn, jiayi.zheng@nudt.edu.cn, jaymaths@nudt.edu.cn

the NNSF in CFTC to achieve the desired formation [23], and it is worth noting that only actuator faults are considered. To accomplish the formation task, Cui et al. used the NNSF in a UAV full-state constraint case [24]. Inspired by the aforesaid work, this paper proposes a fixed-time passive CFTC protocol for multi-UAV, using the NNSF. The pitot tube and actuator faults are considered simultaneously. The main contributions of this paper are as follows:

- 1) A novel fixed-time observer for sensor and actuator faults is proposed. Unlike finite-time convergence [14] or prescribed performance [15] methods that only consider actuator faults, we consider both actuator and sensor faults simultaneously. Unlike the prescribed time control approach that utilizes neural networks for both actuator and sensor faults in [17], [22], we remove the assumption that the faults are bounded in [17], [22] and a general case is considered.
- 2) The norm-normalized sign function (NNSF) is employed to develop the cooperative faults-tolerant control with a smoother control output, and the process of controller design is more streamlined than methods with the sign function [24].

The structure of this paper is: Section II introduces the basics of graph theory, the NNSF, related definitions, and useful lemmas; a fixed-time observer (FTO) is introduced to estimate the sensor and actuator faults, and a CFTC method is developed for formation tracking in Section III; simulations verify the capabilities of the observer and the controller in Section IV. Finally, Section V concludes this paper.

II. PROBLEM FORMULATION AND PRELIMINARIES

A. Graph Theory

Let $\mathcal{G} = (\mathcal{V}, \mathcal{E})$ be the graph describing the topology of the direct communication of N UAVs, where $\mathcal{V} = \{s_1, \dots, s_N\}$ and $\mathcal{E} \subseteq \mathcal{V} \times \mathcal{V}$ represent N nodes and the set of edges connecting each node, respectively. Define $\mathcal{A} = [a_{ij}]_{N \times N}$ to denote the adjacency matrix of the graph \mathcal{G} , where a_{ij} denote the weight coefficients of the edges (s_j, s_i) . When $(s_j, s_i) \in \mathcal{E}$, $a_{ii} = 0$, $a_{ij} > 0$ and vice versa $a_{ij} = 0$. The incidence matrix of the graph \mathcal{G} is $\mathcal{D} = \text{diag}\{\text{deg}_{in}(s_1), \dots, \text{deg}_{in}(s_N)\}$, where $\text{deg}_{in}(s_i) = \sum_{j=1}^N a_{ij}$. Define $\mathcal{L} = [l_{ij}] = \mathcal{D} - \mathcal{A}$ to denote the Laplace matrix of the graph \mathcal{G} , where the elemental values l_{ij} of the Laplace matrix, are expressed as $l_{ii} = \sum_{j=1, j \neq i}^N a_{ij}$ and $l_{ij} = -a_{ij}, i \neq j$.

B. Properties of the Norm-normalized Sign Functions

The expression for the NNSF $\text{sgn}_N(\boldsymbol{\varrho})$ is

$$\text{sgn}_N(\boldsymbol{\varrho}) \triangleq \begin{cases} \frac{\boldsymbol{\varrho}}{\|\boldsymbol{\varrho}\|}, & x \neq 0 \\ 0, & x = 0 \end{cases},$$

where $\boldsymbol{\varrho} = [\varrho_1, \varrho_2, \dots, \varrho_N]^T$. $\|\boldsymbol{\varrho}\|$ is the L_2 norm of $\boldsymbol{\varrho}$.

Since the NNSF is discontinuous and difficult to apply in controller design, it is modified to the following expression as $\text{sgn}_N(\boldsymbol{\varrho})^\chi = \|\boldsymbol{\varrho}\|^\chi \text{sgn}_n(\boldsymbol{\varrho})$, where $\chi > 0$.

C. Related Definitions and Lemmas

Definition 1: For the system, $\dot{\varrho} = h(t, \varrho)$, $\varrho(0) = \varrho_0$, where ϱ is the state of the system and h is a nonlinear function. The initial state of the system is ϱ_0 . If the system is globally finite-time stable and the convergence time function $T(\varrho_0)$ is bounded, then the system's equilibrium is globally fixed-time stable.

Lemma 1: [25] There exists a continuous positive definite unbounded function $V(x)$ such that

$$(1)V(\varrho) = 0 \Leftrightarrow \varrho = 0; (2)\dot{V}(\varrho(t)) \leq -\alpha V^p(\varrho(t)) - \beta V^q(\varrho(t)), \text{ where } \alpha, \beta > 0, p = 1 - \frac{1}{2\lambda}, q = 1 + \frac{1}{2\lambda} \text{ and } \lambda > 1.$$

Then system will be globally stabilized at a fixed time $T \leq T_{\max} = (\pi\lambda)/(\sqrt{\alpha\beta})$.

Lemma 2: [25] Let $\xi_1, \xi_2, \dots, \xi_N \geq 0$.

$$\text{If } 0 < \varkappa < 1, \text{ then } \sum_{i=1}^N \xi_i^\varkappa \geq \left(\sum_{i=1}^N \xi_i\right)^\varkappa.$$

$$\text{If } \varkappa > 1, \text{ then } \sum_{i=1}^N \xi_i^\varkappa \geq N^{1-\varkappa} \left(\sum_{i=1}^N \xi_i\right)^\varkappa.$$

D. Problem Statement

Consider the UAVs have one virtual leader labeled 0 and N followers labeled 1, ..., N in graph \mathcal{G} . The kinematics model of each UAV is

$$\begin{aligned} \dot{x}_i &= v_i \cos \psi_i, \\ \dot{y}_i &= v_i \sin \psi_i, \\ \dot{v}_i &= a_i, \\ \dot{\psi}_i &= \omega_i, \end{aligned} \quad (1)$$

where $\mathbf{p}_i = [x_i, y_i]^T$ denotes the position of the i th UAV. v_i, ψ_i represent the corresponding velocity and the heading angle, respectively. Let $\mathbf{u}_i = [a_i, \omega_i]^T$, where a_i and ω_i are used as the control inputs to represent the acceleration and angular velocity of the UAV, respectively.

Consider the presence of faults, the pitot tube fault of the i th follower is noted as F_{si} , and the loss of efficiency is represented by ρ_i . Then, the sensor and actuator faults model of the i th UAV can be expressed by $v_i^f = v_i + F_{si}$, $\mathbf{u}_i^f = (1 - \rho_i)\mathbf{u}_i$, where v_i^f and \mathbf{u}_i^f represent the airspeed measurement at the fault time and the output control signal of the i th UAV actuator, respectively.

Inspired by [26], the system (1) can be rewritten in the following form

$$\begin{aligned} \dot{\mathbf{p}}_i &= \mathbf{v}_i + \mathbf{f}_{si} + \mathbf{v}_\tau, \\ \dot{\mathbf{v}}_i &= B_i \mathbf{u}_i + B_{fi} \mathbf{u}_i - \rho_i (B_i + B_{fi}) \mathbf{u}_i, \end{aligned} \quad (2)$$

where $\mathbf{v}_\tau = \left[\frac{\bar{v}+v}{2}, \frac{\bar{v}+v}{2}\right]^T$, $\bar{\mathbf{v}}_i = [v_i \cos \psi_i, v_i \sin \psi_i]^T$. $\mathbf{v}_i = \bar{\mathbf{v}}_i - \mathbf{v}_\tau$, \bar{v} and \underline{v} are the upper and lower bounds on the velocity, respectively. $B_i = \begin{bmatrix} \cos \psi_i & -v_i \sin \psi_i \\ \sin \psi_i & v_i \cos \psi_i \end{bmatrix}$, $\mathbf{f}_{si} = \begin{bmatrix} F_{si} \cos \psi_i \\ F_{si} \sin \psi_i \end{bmatrix}$, $B_{fi} = \begin{bmatrix} \cos \psi_i & -F_{si} \sin \psi_i \\ \sin \psi_i & F_{si} \cos \psi_i \end{bmatrix}$, and $0 \leq \rho_i < 1$ is a continuous time-varying function.

Consider the disturbance suffered by the UAV as a centralized disturbance \mathbf{d}_i , which contains the error due to the unmodeled term and the external disturbance, so the centralized disturbance suffered by the i th UAV can be expressed as $\mathbf{d}_i = \Delta \mathbf{a}_i v_i + \mathbf{d}_{vi}$, where $\Delta \mathbf{a}_i$ represents the

error due to the unmodeled term of the system and \mathbf{d}_{vi} is the external disturbance suffered by the i th UAV [27].

Substituting the centralized disturbance into (2) yields the system model (3) when considering the external disturbance as well as the pitot tube and actuator fault

$$\begin{aligned}\dot{\mathbf{p}}_i &= \mathbf{v}_i + \mathbf{f}_{si} + \left[\frac{\bar{v}+v}{2}, \frac{\bar{v}+v}{2} \right]^\top + \mathbf{d}_i, \\ \dot{\mathbf{v}}_i &= B_i \mathbf{u}_i + B_{fi} \mathbf{u}_i - \rho_i (B_i + B_{fi}) \mathbf{u}_i.\end{aligned}\quad (3)$$

It is referred to [27] that we can set $\mathbf{F}_{si} = \mathbf{f}_{si} + \left[\frac{\bar{v}+v}{2}, \frac{\bar{v}+v}{2} \right]^\top + \mathbf{d}_i$, so (3) can be rewritten as

$$\begin{aligned}\dot{\mathbf{p}}_i &= \mathbf{v}_i + \mathbf{F}_{si}, \\ \dot{\mathbf{v}}_i &= B_i \mathbf{u}_i + \mathbf{F}_{ai},\end{aligned}\quad (4)$$

where $\mathbf{F}_{ai} = B_{fi} \mathbf{u}_i - \rho_i (B_i + B_{fi}) \mathbf{u}_i$.

Assumption 1: The derivatives of the pitot tube and actuator faults are both bounded and satisfy $\|\dot{\mathbf{F}}_{si}\| \leq L_1$, $\|\dot{\mathbf{F}}_{ai}\| \leq L_2$, where L_1, L_2 are both known constants.

Remark 1: According to [14], [28], the first order derivatives of the faults are assumed to be bounded here. It should be noted that unlike [17], [22], we do not assume that the faults are bounded, which is also consistent with the laws of operation of real physical systems. Therefore, the conclusions drawn in this paper are more general.

III. MAIN WORK

This paper clearly defines the pitot tube and actuator faults through the previous analysis and fully considers the possible disturbances and unmodeled factors. In this section, we will design a CFTC for the multi-fault case. Firstly, different faults of each UAV are considered as unknown factors and an FTO is designed to estimate multiple faults accurately. Second, the NNSF is used to design the CFTC to achieve formation tracking.

A. FTO Design

Most traditional CFTC methods are limited to handling a single fault or have certain limitations when considering multiple faults. To overcome these limitations, the pitot tube and actuator faults of each UAV are treated as unknown terms and estimated using an FTO. In this subsection, an FTO based on (4) is presented to achieve the differentiation and estimation of the pitot tube and actuator faults to improve the performance and stability of the CFTC.

Theorem 1: For system (4), define $\boldsymbol{\eta}_{i1}$, $\boldsymbol{\eta}_{i2}$, $\boldsymbol{\eta}_{i3}$, and $\boldsymbol{\eta}_{i4}$ as the observer state vectors for the i th UAV and the observer is designed in the following form

$$\begin{cases} \dot{\boldsymbol{\eta}}_{i1} = -k_{i1} \frac{\zeta_{i1}}{\|\zeta_{i1}\|^{\frac{1}{2}}} - k_{i2} \zeta_{i1} \|\zeta_{i1}\|^{\varphi-1} + \boldsymbol{\eta}_{i2} + \mathbf{v}_i, \\ \dot{\boldsymbol{\eta}}_{i2} = -k_{i3} \frac{\zeta_{i1}}{\|\zeta_{i1}\|}, \\ \dot{\boldsymbol{\eta}}_{i3} = -k_{i4} \frac{\zeta_{i2}}{\|\zeta_{i2}\|^{\frac{1}{2}}} - k_{i5} \zeta_{i2} \|\zeta_{i2}\|^{\varphi-1} + \boldsymbol{\eta}_{i4} + \mathbf{u}_i, \\ \dot{\boldsymbol{\eta}}_{i4} = -k_{i6} \frac{\zeta_{i2}}{\|\zeta_{i2}\|}, \end{cases}\quad (5)$$

where $\zeta_{i1} = \boldsymbol{\eta}_{i1} - \mathbf{p}_i$, $\zeta_{i2} = \boldsymbol{\eta}_{i3} - \mathbf{v}_i$, $\zeta_{i1}^s = \boldsymbol{\eta}_{i2} - \mathbf{F}_{si}$, and $\zeta_{i2}^s = \boldsymbol{\eta}_{i4} - \mathbf{F}_{ai}$ are the estimation errors of position, velocity, pitot tube fault, and actuator fault for the i th UAV,

respectively. $\varphi > 0$ is a constant. $\boldsymbol{\eta}_{i2}$ and $\boldsymbol{\eta}_{i4}$ represent estimations of pitot tube and actuator fault of the i th UAV, respectively. If the observer gains k_{i1} , k_{i2} , k_{i3} , k_{i4} , k_{i5} , and k_{i6} satisfy the following conditions, ζ_{i1}^s and ζ_{i2}^s will converge in a fixed time T_i .

$$\begin{cases} 2k_{i2}(\varphi-1)\mathcal{Y}^{\varphi-1/2} > k_{i1} > \sqrt{2k_{i3}}, k_{i2} > 0, k_{i3} > 4L_1, \\ 2k_{i5}(\varphi-1)\mathcal{Y}^{\varphi-1/2} > k_{i4} > \sqrt{2L_1}, k_{i5} > 0, k_{i6} > 4L_2, \end{cases}\quad (6)$$

where $\mathcal{Y} > 0$ is a given constant.

Proof: Substituting the observer (5) into ζ_{i1} and the derivative of ζ_{i1} yields

$$\begin{aligned}\dot{\zeta}_{i1} &= \dot{\boldsymbol{\eta}}_{i1} - \dot{\mathbf{p}}_i \\ &= -k_{i1} \frac{\zeta_{i1}}{\|\zeta_{i1}\|^{\frac{1}{2}}} - k_{i2} \zeta_{i1} \|\zeta_{i1}\|^{\varphi-1} + \zeta_{i1}^s.\end{aligned}\quad (7)$$

Then, we can get

$$\begin{cases} \dot{\zeta}_{i1} = -k_{i1} \frac{\zeta_{i1}}{\|\zeta_{i1}\|^{\frac{1}{2}}} - k_{i2} \zeta_{i1} \|\zeta_{i1}\|^{\varphi-1} + \zeta_{i1}^s, \\ \dot{\zeta}_{i1}^s = -k_{i3} \frac{\zeta_{i1}}{\|\zeta_{i1}\|} - \dot{\mathbf{F}}_{si}. \end{cases}\quad (8)$$

The subsequent proof will be divided into two steps, the first part will demonstrate that $-k_{i2} \|\zeta_{i1}\|^\varphi$ converges to \mathcal{Y} within t_{i1} , and the second part will verify that $-k_{i1} \|\zeta_{i1}\|^{1/2}$ converges to 0 within t_{i2} .

Step 1: Consider $\|\zeta_{i1}(t_0)\| > \mathcal{Y}$. Then, it can be obtained according to the second term in (8) that $\frac{d\|\zeta_{i1}\|}{dt} \leq -k_{i2} \|\zeta_{i1}\|^\varphi$.

Integration of it yields

$$\frac{\|\zeta_{i1}\|^{1-\varphi}}{1-\varphi} \leq -k_{i2}(t-t_0) + \frac{\|\zeta_{i1}(t_0)\|^{1-\varphi}}{1-\varphi} \leq -k_{i2}(t-t_0).\quad (9)$$

Simplification of (9) gives

$$\|\zeta_{i1}\|^\varphi \leq \frac{1}{k_{i2}(\varphi-1)(t-t_0)}.\quad (10)$$

Thus, $\|\zeta_{i1}\|$ will converge to \mathcal{Y} within $t_{i1} \leq t_{i1\max} = \frac{1}{k_{i2}(\varphi-1)\mathcal{Y}^{\varphi-1}}$, where t_{i1} is the convergence time of $-k_{i2} \|\zeta_{i1}\|^\varphi$.

Step 2: At $t > t_{i1}$, $-k_{i2} \|\zeta_{i1}\|^\varphi$ will converge to 0. Therefore, (8) can be rewritten as

$$\begin{cases} \dot{\zeta}_{i1} = -k_{i1} \frac{\zeta_{i1}}{\|\zeta_{i1}\|^{\frac{1}{2}}} + \zeta_{i1}^s, \\ \dot{\zeta}_{i1}^s = -k_{i3} \frac{\zeta_{i1}}{\|\zeta_{i1}\|} - \dot{\mathbf{F}}_{si}. \end{cases}\quad (11)$$

Then, $\frac{d\|\zeta_{i1}\|}{dt} \leq -k_{i1} \|\zeta_{i1}\|^{1/2}$. Integrating it yields

$$\begin{aligned}2\|\zeta_{i1}\|^{1/2} &\leq -k_{i1}(t-t_{i1}) + 2\|\zeta_{i1}(t_{i1})\|^{1/2} \\ &= -k_{i1}(t-t_{i1}) + 2\mathcal{Y}^{1/2}.\end{aligned}\quad (12)$$

Therefore, it can be obtained that at $t_{i2} \leq t_{i2\max} = \frac{2\mathcal{Y}^{1/2}}{k_{i1}}$, $\|\zeta_{i1}\|$ will converge to zero, where $k_{i1} < 2k_{i2}(\varphi-1)\mathcal{Y}^{\varphi-1/2}$ and t_{i2} is the convergence time of $-k_{i1} \|\zeta_{i1}\|^{1/2}$.

Following the proof of Theorem 2 in [29], $\|\zeta_{i1}^s\|$ will converge in a fixed time when $2k_{i2}(\varphi-1)\mathcal{Y}^{\varphi-1/2} > k_{i1} > \sqrt{2k_{i3}}$, $k_{i2} > 0$, and $k_{i3} > 4L_1$.

Similarly, it can be obtained that if the parameters satisfy $2k_{i5}(\varphi-1)\mathcal{T}^{\varphi-1/2} > k_{i4} > \sqrt{2}k_{i6}$, $k_{i5} > 0$, and $k_{i6} > 4L_2$, then, ζ_{i2} and ζ_{i2}^a in observer (5) will also converge in a fixed time.

Therefore, the estimation errors of this observer for the pitot tube and actuator faults will converge in a fixed time T_i , and the proof is complete. ■

B. CFTC Design

Sign functions are commonly used in controller design and play an important role in Lyapunov stability analysis. However, the classical sign function suffers from the problem that easily affected by different types of faults in multi-UAV CFTC, making the control output discontinuity. The introduction of the NNSF can address this challenge effectively, and improve the performance of multi-UAV system.

According to the previous analysis, the i th UAV dynamics model can be rewritten as

$$\begin{aligned}\dot{\boldsymbol{p}}_i &= \boldsymbol{v}_i + \boldsymbol{\eta}_{i2} - \zeta_{i1}^s, \\ \dot{\boldsymbol{v}}_i &= B_i \boldsymbol{u}_i + \boldsymbol{\eta}_{i4} - \zeta_{i2}^a.\end{aligned}\quad (13)$$

Then, we will proceed with the CFTC design. The system will converge in a fixed time regardless of whether the observer converges. Let the virtual velocity of the i th UAV be \boldsymbol{v}_i^v , and the position of the desired trajectory of the formation tracking be \boldsymbol{p}_{di} . $\boldsymbol{\varepsilon}_i = \boldsymbol{p}_i - \boldsymbol{p}_{di}$ represents the error between the i th UAV and the desired trajectory.

Let the velocity error $\boldsymbol{\varsigma}_i$ and tracking error $\boldsymbol{\delta}_i$ of the i th UAV be $\boldsymbol{\varsigma}_i = \boldsymbol{v}_i - \boldsymbol{v}_i^v$, and $\boldsymbol{\delta}_i = \sum_{j=1}^N a_{ij} [(\boldsymbol{p}_i - \boldsymbol{p}_{di}) - (\boldsymbol{p}_j - \boldsymbol{p}_{dj})]$, respectively.

The relative position errors of the above equation can be expressed as $\boldsymbol{\delta} = (\mathcal{L} \otimes I_2)\boldsymbol{\varepsilon}$, where \mathcal{L} , I_2 , and \otimes are the Laplace matrix, the second-order identity matrix, and Kronecker product, respectively. $\boldsymbol{\delta} = [\boldsymbol{\delta}_1^\top, \boldsymbol{\delta}_2^\top, \dots, \boldsymbol{\delta}_N^\top]^\top$, $\boldsymbol{\varepsilon} = [\boldsymbol{\varepsilon}_1^\top, \boldsymbol{\varepsilon}_2^\top, \dots, \boldsymbol{\varepsilon}_N^\top]^\top$.

Inspired by [14], the following virtual input \boldsymbol{v}^v and controller \boldsymbol{u}_i are proposed:

$$\begin{aligned}\boldsymbol{v}^v &= -c_1 \operatorname{sgn}_N[(\mathcal{L} \otimes I_2)\boldsymbol{\varepsilon}]^{\kappa_1} - c_2 \operatorname{sgn}_N[(\mathcal{L} \otimes I_2)\boldsymbol{\varepsilon}]^{\kappa_2} \\ &\quad + \dot{\boldsymbol{p}}_d - \boldsymbol{\eta}_2 + \zeta_{i1}^s,\end{aligned}\quad (14)$$

$$\begin{aligned}\boldsymbol{u}_i &= B_i^{-1} [-c_3 \operatorname{sgn}_N(\boldsymbol{\varsigma}_i)^{\kappa_1} - c_4 \operatorname{sgn}_N(\boldsymbol{\varsigma}_i)^{\kappa_2} - \boldsymbol{\eta}_{i4} \\ &\quad + \zeta_{i2}^a + \dot{\boldsymbol{v}}_i^v - (\mathcal{L} \otimes I_2)\boldsymbol{\varepsilon}],\end{aligned}\quad (15)$$

where c_1 , c_2 , c_3 , and c_4 are positive constants. $0 < \kappa_1 < 1$, $1 < \kappa_2 < 2$, $\boldsymbol{v}^v = [\boldsymbol{v}_1^v, \boldsymbol{v}_2^v, \dots, \boldsymbol{v}_N^v]^\top$, $\dot{\boldsymbol{p}}_d = [\dot{\boldsymbol{p}}_{d1}, \dot{\boldsymbol{p}}_{d2}, \dots, \dot{\boldsymbol{p}}_{dN}]^\top$, and $\boldsymbol{\eta}_2 = [\boldsymbol{\eta}_{12}, \boldsymbol{\eta}_{22}, \dots, \boldsymbol{\eta}_{N2}]^\top$, where the elements in $\boldsymbol{\eta}_2$ are estimations of sensor fault.

Theorem 2: Under observer (5), virtual inputs (14), and controller (15), the multi-UAV (13) can realize the CFTC in a fixed time.

Proof: Consider the Lyapunov function $V_1 = \frac{1}{2}\boldsymbol{\varepsilon}^\top (\mathcal{L} \otimes I_2)\boldsymbol{\varepsilon}$. Derivation of V_1 gives

$$\dot{V}_1 = [(\mathcal{L} \otimes I_2)\boldsymbol{\varepsilon}]^\top (\boldsymbol{v} + \boldsymbol{\eta}_2 - \zeta_{i1}^s - \dot{\boldsymbol{p}}_d), \quad (16)$$

where $\boldsymbol{v} = [\boldsymbol{v}_1^\top, \boldsymbol{v}_2^\top, \dots, \boldsymbol{v}_N^\top]^\top$. It is worth noting that the estimation error ζ_{i1}^s of observer is included in the Lyapunov

function, i.e., the UAVs can achieve convergence even when the observer has not yet converged.

Let $\boldsymbol{\varsigma} = [\boldsymbol{\varsigma}_1^\top, \boldsymbol{\varsigma}_2^\top, \dots, \boldsymbol{\varsigma}_N^\top]^\top$, then, $\boldsymbol{v} = \boldsymbol{\varsigma} + \boldsymbol{v}^v$. Substituting this into (16) yields

$$\dot{V}_1 = [(\mathcal{L} \otimes I_2)\boldsymbol{\varepsilon}]^\top (\boldsymbol{\varsigma} + \boldsymbol{v}^v + \boldsymbol{\eta}_2 - \zeta_{i1}^s - \dot{\boldsymbol{p}}_d). \quad (17)$$

Substituting the NNSF and (14) while applying Lemma 2 yields

$$\begin{aligned}\dot{V}_1 &\leq -c_1 \|(\mathcal{L} \otimes I_2)\boldsymbol{\varepsilon}\|^{\kappa_1+1} - c_2 \|(\mathcal{L} \otimes I_2)\boldsymbol{\varepsilon}\|^{\kappa_2+1} \\ &\quad + [(\mathcal{L} \otimes I_2)\boldsymbol{\varepsilon}]^\top (\boldsymbol{\varsigma} + \dot{\boldsymbol{p}}_d - \dot{\boldsymbol{p}}_d) \\ &\leq -c_1 \tau_1 V_1^{\frac{\kappa_1+1}{2}} - c_2 \tau_2 V_1^{\frac{\kappa_2+1}{2}} + [(\mathcal{L} \otimes I_2)\boldsymbol{\varepsilon}]^\top \boldsymbol{\varsigma},\end{aligned}\quad (18)$$

where $\tau_1, \tau_2 > 0$.

Then, select the Lyapunov function $V_2 = \frac{1}{2} \sum_{i=1}^N \boldsymbol{\varsigma}_i^\top \boldsymbol{\varsigma}_i$. Derivation of it gives

$$\dot{V}_2 = \sum_{i=1}^N \boldsymbol{\varsigma}_i^\top (B_i \boldsymbol{u}_i + \boldsymbol{\eta}_{i4} - \zeta_{i2}^a - \dot{\boldsymbol{v}}_i^v). \quad (19)$$

The UAV's velocity is not 0 during the practical flight, then $\det(B_i) = v_i \cos^2 \psi_i + v_i \sin^2 \psi_i \neq 0$.

Therefore, substitute (15) into (19). It can be obtained that

$$\begin{aligned}\dot{V}_2 &= \sum_{i=1}^N \boldsymbol{\varsigma}_i^\top \{-c_3 \operatorname{sgn}_N(\boldsymbol{\varsigma}_i)^{\kappa_1} - c_4 \operatorname{sgn}_N(\boldsymbol{\varsigma}_i)^{\kappa_2} - \boldsymbol{\eta}_{i4} + \zeta_{i2}^a \\ &\quad + \dot{\boldsymbol{v}}_i^v - [(\mathcal{L} \otimes I_2)\boldsymbol{\varepsilon}] + \boldsymbol{\eta}_{i4} - \zeta_{i2}^a - \dot{\boldsymbol{v}}_i^v\} \\ &\leq -c_3 \tau_3 V_2^{\frac{\kappa_1+1}{2}} - c_4 \tau_4 V_2^{\frac{\kappa_2+1}{2}} - [(\mathcal{L} \otimes I_2)\boldsymbol{\varepsilon}]^\top \boldsymbol{\varsigma},\end{aligned}\quad (20)$$

where $\tau_3, \tau_4 > 0$.

Finally, consider the combined Lyapunov function $V = V_1 + V_2$. According to (18)(20), we have

$$\begin{aligned}\dot{V} &\leq -c_1 \tau_1 V_1^{\frac{\kappa_1+1}{2}} - c_2 \tau_2 V_1^{\frac{\kappa_2+1}{2}} + [(\mathcal{L} \otimes I_2)\boldsymbol{\varepsilon}]^\top \boldsymbol{\varsigma} \\ &\quad - c_3 \tau_3 V_2^{\frac{\kappa_1+1}{2}} - c_4 \tau_4 V_2^{\frac{\kappa_2+1}{2}} - [(\mathcal{L} \otimes I_2)\boldsymbol{\varepsilon}]^\top \boldsymbol{\varsigma} \\ &\leq -\iota_1 V^{\frac{\kappa_1+1}{2}} - \iota_2 V^{\frac{\kappa_2+1}{2}},\end{aligned}\quad (21)$$

where $\iota_1 = \min\{c_1 \tau_1, c_3 \tau_3\}$, $\iota_2 = \min\{c_2 \tau_2, c_4 \tau_4\}$, $0 < \kappa_1 < 1$, $1 < \kappa_2 < 2$.

Let $\mu_c = \frac{1}{1-\kappa_1}$. Then, it follows from Lemma 1 that the system will converge in a fixed time $T \leq T_{\max} = \frac{\pi}{\mu_c \sqrt{\iota_1 \iota_2}}$, and the proof is complete. ■

Remark 2: The introduction of the NNSF allows the proof process to be compact. Meanwhile compared to the classical sign function, the NNSF makes the controller proof process smoother, i.e., it divides the original basis by the norm of the vector instead of directly setting it to 1 or -1.

IV. NUMERICAL SIMULATION

In this section, a succession of numerical simulations will be presented to verify the validity of the proposed CFTC. Consider that there are four UAVs, and their topological relationship is shown in Fig. 1.

The velocity $v_i(0)$ are 25m/s, 22m/s, 17m/s, and 21m/s, respectively. The initial positions of UAVs

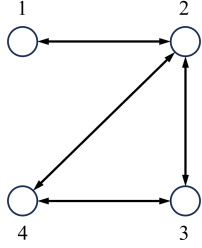


Fig. 1. Topology of the UAV swarm.

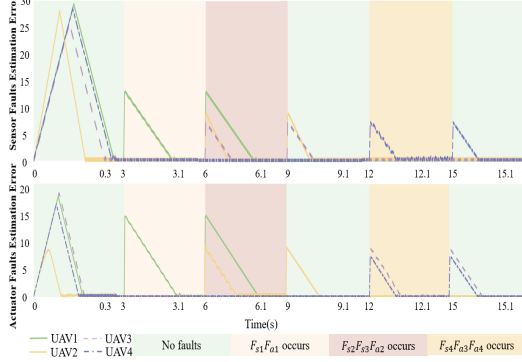


Fig. 2. Estimation of FTO.

are $[42m, -10m]^T$, $[86m, -1m]^T$, $[95m, 90m]^T$, and $[53m, 69m]^T$. Then, the heading angle are $\frac{\pi}{4}$, $\frac{\pi}{3}$, $\frac{\pi}{2}$, and 0, respectively.

A. Observer Performance

Pitot tube and actuator faults at different periods are $F_{s1} = 10 + 0.1 \sin(t)(3 < t \leq 6)$, $F_{s2} = 12 + 0.3 \sin(t)(6 < t \leq 9)$, $F_{s3} = 8 + 0.5 \cos(t)(6 < t \leq 9)$, $F_{s4} = 12 + 0.2 \cos(t)(9 < t \leq 12)$, $F_{a1} = 15 + 0.1 \sin(t)(3 < t \leq 6)$, $F_{a2} = 6 + 0.3 \cos(t)(6 < t \leq 9)$, $F_{a3} = 12 + \cos(t)(12 < t \leq 15)$, $F_{a4} = 9 + 0.2 \cos(t)(12 < t \leq 15)$, and no faults occur at the remaining moments.

Since the observer converges rapidly, we use a non-isometric timeline to show the performance of the observer for ease of visualization. Through Fig. 2, we can find that the observer converges in $0.3s$ without faults. As mentioned above, this subsection is designed with different sensor and actuator faults at different time periods, each of which has a duration of $3s$. According to Fig. 2, it can be identified that the convergence of the observer error can be achieved within $0.1s$ after the faults occur. It should also be noted that although no faults are imposed on the system in $12s - 15s$, there exists faults before $12s$, so the sudden disappearance of the faults also generates some fluctuations. It can be demonstrated from Fig. 2 that the FTO proposed in this paper has promising performance and can estimate different faults well.

B. Controller Performance

In this subsection, we contrast the proposed controller with the existing approach [14], and the results are depicted in two dimensions. The acceleration and angular velocity for the desired trajectory of each UAV are $a_i = 4 \cos(0.44t)$

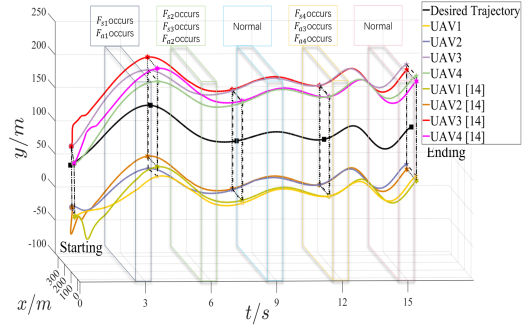


Fig. 3. Trajectory of each UAV.

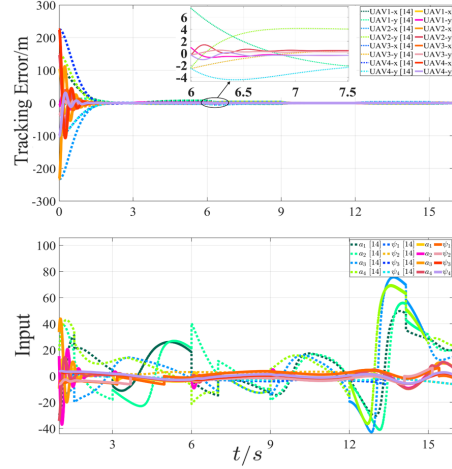


Fig. 4. Tracking error and inputs of each UAV.

and $\omega_i = \sin(0.007t)$, respectively. The trajectories of the multi-UAV are shown in Fig. 3.

The black line is the desired trajectory of the UAV formation, according to Fig. 3, it can be found that both the CFTC proposed in this paper and the controller in [14] can realize multi-UAV formation fault-tolerant control in a fixed time. However, it should be noted that in the initial stage, the method in [14] has a tendency to diverge, compared to the method presented in this paper, which is smoother. Meanwhile, since this paper introduces the NNSF in the controller design, it makes the output of the controller less affected by faults. Intuitively, one can observe the Z-axis in Fig. 3, which represents the offset of the UAV in the Y-direction, and when a fault occurs, it can be found that the control output of [14] has an obvious offset in the Y-direction, compared to the controller designed with the NNSF of this paper which has a much improved performance and the formation tracking process is smoother. The relative position error δ and control inputs of the UAVs are shown in Fig. 4.

Simulation results show that both methods can achieve convergence of the tracking error. However, the CFTC proposed in this paper is less affected by faults. As an instance, the system suffers from both sensor and actuator faults meanwhile in $6s - 9s$. In the diagram of tracking error, in the series of $6s$ to $7.5s$, the method proposed in [14] suffers

from faults more obviously ($-4m$ to $6m$), compared to the CFTC proposed in this paper, which can guarantee that the tracking error fluctuates in a tiny range ($-2m$ to $2m$) and convergence of tracking error can be achieved in $1.5s$. In the diagram of the control inputs, it can be seen that compared to [14], the CFTC proposed in this paper is smoother both in terms of angular velocity and acceleration, which well validates the effectiveness of introducing a norm-normalized sign function in the controller, i.e., to enable the system's control inputs to be smoother.

V. CONCLUSIONS

In this paper, the formation control problem of multi-UAV when facing sensor and actuator faults is investigated. By introducing an FTO, the estimation errors for different faults converge in a fixed time. Then, the NNSF is employed in controller design to realize fast convergence of the multi-UAV in a fixed time. Additionally, the incorporation of the NNSF mitigates the impact of pitot tube and actuator faults on the control output of the multi-UAV system. As a result, the UAV is able to maintain a stable flight trajectory, ensuring smooth and uninterrupted operation. Finally, the performance of the proposed CFTC is demonstrated through a series of simulations.

REFERENCES

- [1] X. Chen, J. Zheng, and Q. Hu. A Hybrid Planning Method for 3D Autonomous Exploration in Unknown Environments With a UAV. *IEEE Transactions on Automation Science and Engineering*, pp. 1–12, 2023.
- [2] D. D. Oh, D. Lee, and H. J. Kim. Safety-Critical Control Under Multiple State and Input Constraints and Application to Fixed-Wing UAV In 2023 62nd IEEE Conference on Decision and Control (CDC), pp. 1748–1755, 2023.
- [3] F. Liu, S. Yuan, W. Meng, R. Su, and L. Xie. Multiple Noncooperative Targets Encirclement by Relative Distance-Based Positioning and Neural Antisynchronization Control. *IEEE Transactions on Industrial Electronics*, vol. 71, no. 2, pp. 1675–1685, 2024.
- [4] M. L. Fravolini, G. Del Core, U. Papa, P. Valigi, and M. R. Napolitano. Data-Driven Schemes for Robust Fault Detection of Air Data System Sensors. *IEEE Transactions on Control Systems Technology*, vol. 27, no. 1, pp. 234–248, 2019.
- [5] R. McCloy, J. De Doná, and M. Seron. Sensor switching fault tolerant MPC for constrained LPV systems. In 2017 IEEE 56th Annual Conference on Decision and Control (CDC), pp. 6377–6382, 2017.
- [6] Z. Wang, L. Liu, and H. Zhang. Neural Network-Based Model-Free Adaptive Fault-Tolerant Control for Discrete-Time Nonlinear Systems With Sensor Fault. *IEEE Transactions on Systems, Man, and Cybernetics: Systems*, vol. 47, no. 8, pp. 2351–2362, 2017.
- [7] A. Abbaspour, K. Yen, P. Forouzannezhad, and A. Sargolzaei. A Neural Adaptive Approach for Active Fault-Tolerant Control Design in UAV. *IEEE Transactions on Systems, Man, and Cybernetics: Systems*, vol. 50, no. 9, pp. 3401–3411, 2020.
- [8] B. Gao, Y. Liu, and L. Liu. Adaptive neural fault-tolerant control of a quadrotor UAV via fast terminal sliding mode. *Aerospace Science and Technology*, vol. 129, pp. 107818, 2022.
- [9] L. Wang, H. Wang, and P.X. Liu. Finite-Time Compensation Control for State-Variable-Unmeasurable Nonlinear Systems With Sensor and Actuator Faults. *IEEE Transactions on Instrumentation and Measurement*, vol. 71, pp. 1–8, 2022.
- [10] J. Han, X. Liu, X. Xie, and X. Wei. Dynamic Output Feedback Fault Tolerant Control for Switched Fuzzy Systems With Fast Time Varying and Unbounded Faults. *IEEE Transactions on Fuzzy Systems*, vol. 31, no. 9, pp. 3185–3196, 2023.
- [11] Z. Yang, B. Yang, R. Ji, and J. Ma. Adaptive Finite Time Prescribed Performance Fault Tolerant Control for Spacecraft Attitude Maneuver. In 2023 62nd IEEE Conference on Decision and Control (CDC), pp. 5863–5868, 2023.
- [12] Y. Liu, X. Dong, P. Shi, Z. Ren, and J. Liu. Distributed Fault-Tolerant Formation Tracking Control for Multiagent Systems With Multiple Leaders and Constrained Actuators. *IEEE Transactions on Cybernetics*, vol. 53, no. 6, pp. 3738–3747, 2023.
- [13] Y. Zhong, G. Lyu, X. He, Y. Zhang, and S.S. Ge. Distributed Active Fault-Tolerant Cooperative Control for Multiagent Systems With Communication Delays and External Disturbances. *IEEE Transactions on Cybernetics*, vol. 53, no. 7, pp. 4642–4652, 2023.
- [14] W. Cheng, K. Zhang, B. Jiang, and S.X. Ding. Fixed-Time Fault-Tolerant Formation Control for Heterogeneous Multi-Agent Systems With Parameter Uncertainties and Disturbances. *IEEE Transactions on Circuits and Systems I: Regular Papers*, vol. 68, no. 5, pp. 2121–2133, 2021.
- [15] W. Cheng, K. Zhang, and B. Jiang. Fixed-Time Fault-Tolerant Formation Control for a Cooperative Heterogeneous Multiagent System With Prescribed Performance. *IEEE Transactions on Systems, Man, and Cybernetics: Systems*, vol. 53, no. 1, pp. 462–474, 2023.
- [16] Y. Li, S. Dong, K. Li, and S. Tong. Fuzzy Adaptive Fault Tolerant Time-Varying Formation Control for Nonholonomic Multirobot Systems With Range Constraints. *IEEE Transactions on Intelligent Vehicles*, vol. 8, no. 6, pp. 3668–3679, 2023.
- [17] J. Han, J. Zhang, C. He, C. Lv, X. Hou, and Y. Ji. Distributed Finite-Time Safety Consensus Control of Vehicle Platoon With Sensor and Actuator Failures. *IEEE Transactions on Vehicular Technology*, vol. 72, no. 1, pp. 162–175, 2023.
- [18] Y. Zou, H. Zhang, and W. He. Adaptive Coordinated Formation Control of Heterogeneous Vertical Takeoff and Landing UAVs Subject to Parametric Uncertainties. *IEEE Transactions on Cybernetics*, vol. 52, no. 5, pp. 3184–3195, 2022.
- [19] G. Perozzi, A. Polyakov, F. Miranda-Villatoro, and B. Brogliato. Upgrading linear to sliding mode feedback algorithm for a digital controller. In 2021 60th IEEE Conference on Decision and Control (CDC), pp. 2059–2064, 2021.
- [20] Zehui Mao, Xing-Gang Yan, Bin Jiang, and Sarah K. Spurgeon. Sliding Mode Control of Nonlinear Systems With Input Distribution Uncertainties. *IEEE Transactions on Automatic Control*, vol. 68, no. 10, pp. 6208–6215, 2023.
- [21] D. Li, S.S. Ge, and T. H. Lee. Fixed-Time-Synchronized Consensus Control of Multiagent Systems. *IEEE Transactions on Control of Network Systems*, vol. 8, no. 1, pp. 89–98, 2021.
- [22] W. Cheng, K. Zhang, B. Jiang, and S. Simani. Neural Network Observer-Based Prescribed-Time Fault-Tolerant Tracking Control for Heterogeneous Multiagent Systems With a Leader of Unknown Disturbances. *IEEE Transactions on Aerospace and Electronic Systems*, vol. 59, no. 6, pp. 9042–9053, 2023.
- [23] K. Yan, T. Han, B. Xiao, and H. Yan. Energy-Constraint Adaptive Time-Varying Formation Tracking for Multi-Agent Systems With Multiple Leaders and Bounded Unknown Inputs. *IEEE Transactions on Circuits and Systems II: Express Briefs*, vol. 71, no. 2, pp. 802–806, 2024.
- [24] G. Cui, H. Xu, X. Chen, and J. Yu. Fixed-Time Distributed Adaptive Formation Control for Multiple QUAUVs With Full-State Constraints. *IEEE Transactions on Aerospace and Electronic Systems*, vol. 59, no. 4, pp. 4192–4206, 2023.
- [25] X. Wei, W. Yu, H. Wang, Y. Yao, and F. Mei. An Observer-Based Fixed-Time Consensus Control for Second-Order Multi-Agent Systems With Disturbances. *IEEE Transactions on Circuits and Systems II: Express Briefs*, vol. 66, no. 2, pp. 247–251, 2019.
- [26] J. Zheng, S. Zhao, Q. Wang, X. Wang, and H. Zhou. Adaptive Prescribed-Time Tracking Control for Fixed-Wing UAV with the Input Saturation and State Constraints. In 2023 62nd IEEE Conference on Decision and Control (CDC), pp. 3561–3566, 2023.
- [27] Y. Li, C. Wang, J. Liu, J. Wang, and Z. Zuo. Formation containment control of multi-agent systems with actuator and sensor faults. *International Journal of Robust and Nonlinear Control*.
- [28] Z. Ye, B. Jiang, Y. Cheng, Z. Yu, and Y. Yang. Distributed fault diagnosis observer for multi-agent system against actuator and sensor faults. *Journal of Systems Engineering and Electronics*, vol. 34, no. 3, pp. 766–774, 2023.
- [29] M. Basin, C. Bharath Panathula, and Y. Shtessel. Multivariable continuous fixed-time second-order sliding mode control: design and convergence time estimation. *IET Control Theory & Applications*, vol. 11, no. 8, pp. 104–1111, 2017.